LEGIBILITY NOTICE

A major purpose of the Technical Information Center is to provide the broadest dissemination possible of information contained in DOE's Research and Development Reports to business, industry, the academic community, and federal, state and local governments.

Although a small portion of this report is not reproducible, it is being made available to expedite the availability of information on the research discussed herein.

Los Alamos National Laboratory is operated by the University of California for the United States Department of Energy under contract W-7405-ENG-36

TITLE: SHOCK WAVE EFFECTS AND METALLURGICAL PARAMETERS

LA-UR--87-1609

DE87 010115

AUTHOR(S): Karl Paul Staudhammer, MST-7

SUBMITTED TO: International Conference on Impact Loading and Dynamic Behavior of Materials
Bremen, West Germany
May 18-22, 1987

DISCLAIMER

This report was prepared as an account of work sponsored by an agency of the United States Government. Neither the United States Government nor any agency thereof, nor any of their employees, makes any warranty, express or implied, or assumes any legal liability or responsibility for the accuracy, completeness, or usefulness of any information, apparatus, product, or process disclosed, or represents that its use would not infringe privately owned rights. Reference herein to any specific commercial product, process, or service by trade name, trademark, manufacturer, or otherwise does not necessarily constitute or imply its endorsement, recommendation, or favoring by the United States Government or any agency thereof. The views and opinions of authors expressed herein do not necessarily state or reflect those of the United States Government or any agency thereof.

By acceptance of this article, the publisher recognizes that the U S Government retains a nonexclusive, royalty-free license to publish or reproduce the published form of this contribution, or to allow others to do so, for U S Government purposes

The Los Alamos National Laboratory requests that the publisher identify this article as work performed under the auspices of the U S Department of Energy

Los Alamos Los Alamos National Laboratory
Los Alamos, New Mexico 87545

FORM NO 836 R4

Shock Wave Effects and Metallurgical Parameters

K. P. Staudhammer, Materials Science and Technology Division, Los Alamos, New Mexico, USA

Introduction

The metallurgical effects associated with dynamic loading were first described by Reinhart and Pearson (1). The first systematic investigation of the substructural changes induced by the passage of shock waves is described by C. Smith (2). During the past three decades, the number of publications has in essence exponentially continued, with now, one, two, or more major shock conferences per year. The earlier work in shock loading consisted primarily of studies devoted to the determination of residual structures, substructures, and mechanical properties on materials having reasonable ductilities, i.e., metals and alloys. Concommitant to these studies was the realization that shock wave parameters do effect the substructure and associated mechanical properties. Largely, this interdependence of shock wave and metallurgical parameters arose from the obvious and significant disagreements among investigators, and have been attributed to variations in experimentation and ill defined pre/post shock conditions of both the shock physics and metallurgical characterization, some of which confusion still exists to date. Consequently, a fundamental understanding has been difficult. Recently, we have found that residual microstructures are not only significant to the shock physics, but that many metallurgical parameters are interdependent with one another.

This paper will focus on the metallurgical features produced by the passage of shock waves in metals. The microstructural changes thus produced and their attendant effects on physical properties, primarily the mechanical properties discussed here, have been more eminently investigated in the past decades (3-10). It has been shown that dislocations, dislocation cells, planar dislocation arrays, stacking faults, twins, twin-faults and point defects, all contribute specifically or in many instances concommitantly in metal-alloy systems to residual shock strengthening. These shock induced microstructures are for the most part governed by the stacking fault free energy. Stacking fault free energies largely control the movement and subsequent arrangement of dislocations and contribute to the production of other crystal defects or phase changes (11). High stacking fault free energy metals and alloys such as nickel are characterized by dislocation cell structures; while low staking fault free energy metals and alloys such as 304 stainless steel (in fcc structures) are characterized by planar dislocation arrays, stacking faults and twins. These parameters have been identified, and their effects have been documented (7, 9). Consequently, affecting the residual microstructure, these parameters also affect the residual mechanical properties. Of significant importance, and becoming more visible in shock experimentation, particularly in light of the increase in very high pressure work, is the contribution of strain to the overall residual properties. While strain (deformation) effects were known for some time, elimination of this strain was sought via appropriate momentum trapping. However, as no material is a perfect metallurgical system, complete elimination was not and is not yet possible. At best a minimization of this strain can be achieved. Fortuitously, at low pressures (i.e., 25 GPa for most metals) this associated strain was indeed considered to be negligible. Nonetheless, for higher pressure improperly momentum trapped experiments,

MASTER DISTRIBUTION OF THIS DOCUMENT IS UNLIMITED

the strain became a major contributor to the overall residual structure-properties. These effects were beginning to be discussed in the literature as a contributed major effect of the shock phenomena (16, 17). Additionally, the effect of strain rate, particularly at explosively driven strain rates, on deformation mechanisms in materials, is of fundamental interest. For many metals the strain rate sensitivity is known to increase quite dramatically when strain rates increase above 10^3/s (18, 19). Thus, deformation by dislocation motion, which is a thermally activated mechanism, is strain rate dependent and more significant at the shock velocities (i.e., $\sim 10^6$/s) used in explosive systems discussed here.

Shock Wave Parameters

The calculation of shock wave parameters is based in its simplest form on the Rankine-Hugoniot equations. A "how-to" guide for the design of shock loading flyer plate systems is given in (20). The parameters necessary for producing given pressures and pulse durations along with their associated temperature effects are also elaborated on in (21) and will not be presented here except to highlight their consequence on the residual microstructure. Illustrated in Figure 1 is a schematic of a typical pressure-time profile of a shock event. The particulars of this figure are discussed below.

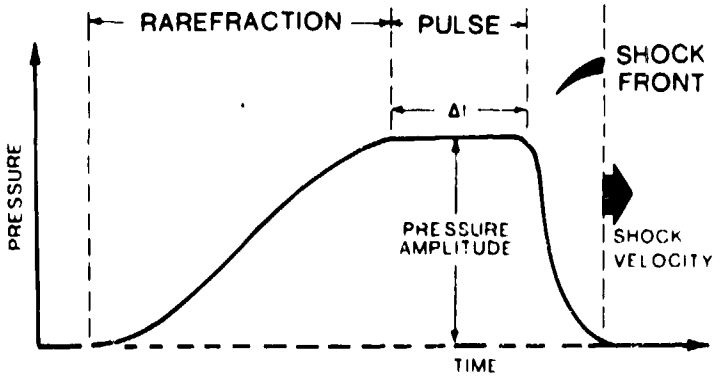

Fig. 1: Schematic of shock wave profile.

A. Strain Rate: The strain rates discussed in this paper are in the range of 10^5-10^6/s. The are generated via high explosive detonation and are discussed in sufficient detail elsewhere (20).

B. Pressure: The pressure imparted on a system is calculated by a technique called impedence matching. A detailed description is given in (20) wherein pressures can be obtained for a wide range of materials and for flyer plate experiments, used for pressures up to megabars.

A direct consequence of pressure on shocked metals is the increase in hardness with increasing pressure as evident by the numerous observations on a wide variety of materials (6, 11, 22). However, with increasing pressures the hardness levels off and actually decreases at very high pressure (>100 GPa). This decrease has been attributed mainly to shock heating effects which will be discussed later.

C. Pulse duration: The effects of pulse duration are principally to allow for time dependent events to occur for sufficient magnitude shock pressure. Short pulse durations i.e.; less than 0.25 μs, for some materials and 0.1 μs for most, appear to be too short of a duration for equilibrium substructures to develop. While some investigators (21, 22) have observed dislocation density increases with increasing pulse duration in the nanosecond range, they are, however in question due to pressure variations. For pulse durations in excess of 0.5 μs up to 20 μs most materials with sufficient pressures have saturated substructural effects which are essentially pulse duration independent (23). The saturation levels will, of course, vary with many metallurgical parameters.

D. Temperature: Thermal effects are associated with the passage of a shock wave. The thermal effects arise from different phenomena. Initially from shock compression, an adiabatic temperature rise proportional to the shock pressure and shock conditions is generated. If the shock wave traverses a sample obeying hydrodynamic laws (i.e., no shear strength) the temperature rise during the shock pulse can be calculated from the Rankine-Hugoniot relationships (20). Upon return to ambient pressure, the entropic (irreversibility) nature of the process causes the residual temperature to have increased over that of the ambient condition. This residual (entropic) temperature rise in stainless steel as a function of pressure is shown in Figure 2.

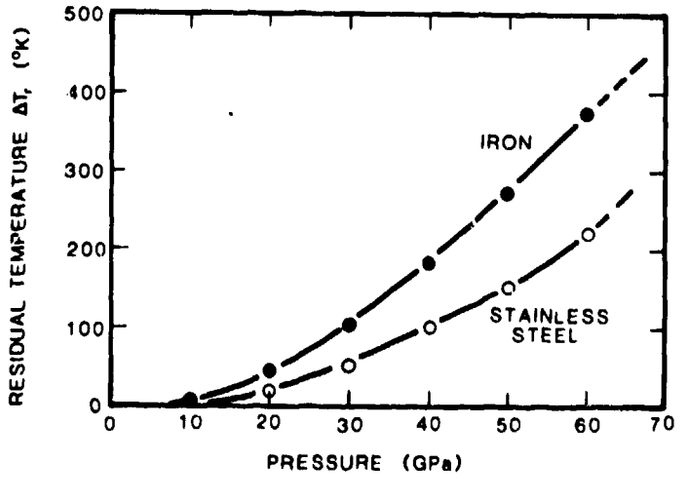

Fig. 2: Residual temperature for iron and stainless steel as a function of pressure. Data from (16).

Thus, temperature has several sources in a shock event. The intrinsic temperature arising from the shock event is attributed to the adiabatic temperature and is a function of the pressure. Added to this is the entropic (residual) temperature and strain heat resulting from deformation (this will be discussed in more detail later). Of course, one must account for the initial temperature at which the shock event is initiated. Consequently, one should not only compare temperature but more appropriately the homologous temperature (T/Tm). This is of particular importance for comparison of materials with widely varying melting points.

Metallurgical Parameters

The substructures generated by shock events depend not only upon shock wave conditions, but material parameters as well. The importance of metallurgical parameters of any system subject to shock events cannot be overemphasized. For shock wave conditions the pressure appears to be the most dominant effect, while for material parameters (viewed in terms of mechanical advantage) a host of structural (macro and micro) features both intrinsic (i.e., stacking fault free energy) and extrinsic (i.e., grain size) in nature interact and control the response of the material. Consequently, the resulting structures which affect the properties of a post shocked sample are indeed complex and more often a contributive effect of more than one parameter. These parameters have been identified, and their effects have been investigated. Thus, by altering the residual microstructure these parameters in turn also affect the residual properties.

A. Pre-existing microstructure: In many early experiments, pre-metallurgical conditions, as well as shock conditions, were not specified. It is now known (24) that grain size can have a significant effect on residual hardness of shock-loaded materials.

If the shock event has sufficient pressure and duration, the resultant effect on the microstructure may overshadow/overcome any pre-existing microstructure. However, as residual microstructures are observed and documented, one must comprehend the full microstructural evolution which generally is not the same for varied prestructures. Ideally, one must account for or minimize such parameters as dislocation density, texturing, and grain size variations. Materials with pre-existing substructures and subsequent shock events were investigated by Murr (23) and Staudhammer (25). They found that the pre-existing micro- structure altered the residual properties. These investigations also showed that deformation sequencing (i.e., cold worked and then shocked or shocked then cold worked) or multiple duration effects (shocked 3 times 2 μs versus one at 6 μs) produced different results in hardness.

B. Point defects: Because of the very high strain rates associated with shock loading, a high density of point defects (both vacancies and interstitial) normally occurs. Traditionally, point defects have been difficult to characterize in shock-induced microstructures. The only direct observations of point defects produced by shock events were made by Murr, et. al. (11) on shock-loaded molybdenum using field ion microscopy shown in Figure 3. Prior to this, resistivity measurements were the tool of choice, for example, as illustrated in Figure 4, several investigators (26-30) systematically have shown that with an increase in shock deformation, point defects increase.

While point defects contributed to the hardening in molybdenum, it is inconclusive to extend this to other materials. Clearly these types of experiments need further work on a variety of materials to further elucidate the point defect contribution. Point defects can cluster and form vacancy loops as well as interstitial loops. The implication of point defects as precursors to other higher order substructures is of particular importance to shock-induced microstructures.

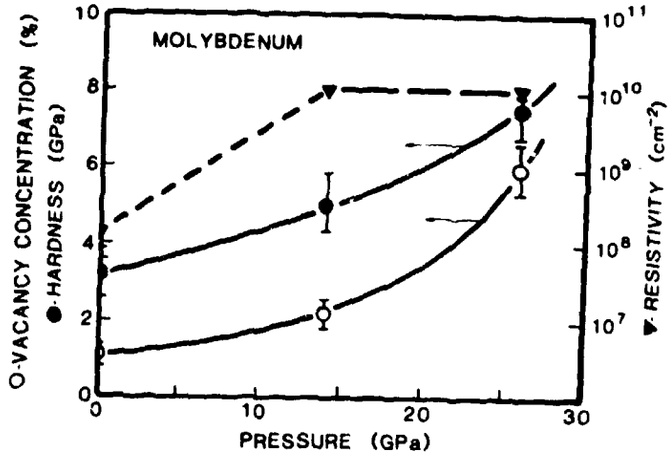

Fig. 3: Shock-induced vacancies and hardness in molybdenum vs. pressure, after Murr, et. al. (34).

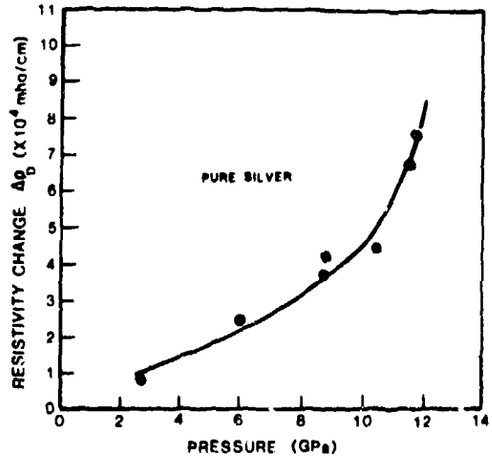

Fig. 4: Resistivity changes in shock loaded silver. At 12 GPa the vacancy concentration equaled 2 x 10^{-3}. Data of Dick, et. al (23).

These point defect clusters are somewhat better understood than point defects, and can be observed via transmission electron microscopy. However, both point defects and point defect clusters are obscured by other shock induced microstructures (discussed later) particularly at high pressures and/or high strains.

C. Dislocation densities: Dislocation structures while dependent upon stacking fault free energy and other dynamic considerations are also dependent upon the dislocations generated by the applied stress and the available time to move them. Typically, for pulse durations in excess of 0.1 μs, the dislocation density increases with pressure (25). This is shown in Figure 5 for 304 and 316 stainless steel, at a pulse duration of 2 μs. For materials having high stacking fault free energies, greater than 60 mJ/m^2, dislocation cell structures are formed. For stacking fault free energies below about 40 mJ/m^2 planar arrays of dislocations, stacking faults and other planar

microstructures result. For stacking fault energies between 40-60 mJ/m^2 a transitional microstructure is usually observed. Not all materials show the same dislocation structures for given shock conditions. For example, the number of available slip systems for bcc and fcc materials are not the same. The predominant microstructural features in bcc materials are tangles and cell like structures.

Dislocation cells are the predominant equilibrium structures for high stacking fault materials. The main consideration in forming cells as equilibrium arrays depends upon the dislocations generated as well as the pulse duration. Dislocation cells are characterized by cell dimensions, wall size and structure. As a result, in shock loaded materials the dislocation cell size is largely a function of peak pressure, while the wall and cell structure are influenced to some extent by the pulse duration. For peak pressures in excess of approximately 35 GPa and dependent upon shock design, associated strains are present (30). These strains, which normally increase with pressure, can and do greatly influence the residual microstructure. The strain effect will be elaborated on later when combined effects are discussed.

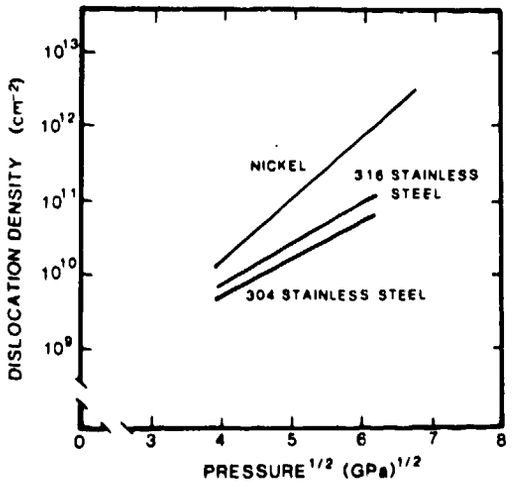

Fig. 5. Dislocation density as a function of peak shock pressure for nickel, 316 and 304 stainless steel. Nickel data after Murr (11) and stainless steel data after Staudhammer (21).

For all high stacking fault free energy materials, the dislocation cell size decreases with increasing shock pressure. Examples are shown in Figure 6. Figure 7 illustrates the effects of both pressure (strain) and experimental variation, the cylindrical lens having a higher pressure and associated strain than the flyer plate data. At higher pressures elongated cells and twins were observed. These are shown in Figure 8. Additionally, Murr (11) has found that there is a grain size effect on dislocation cell size of shock-loaded nickel, and that a relationship exists between dislocation cell size and the square root of dislocation density as shown in Figure 9.

Cell size is considerably different in shock loaded aluminum, Figure 10, from those observed for more conventional deformation at equivalent strains. This was also observed in nickel by Zimmer (31) and further elaborated on by Murr, et. al. (11).

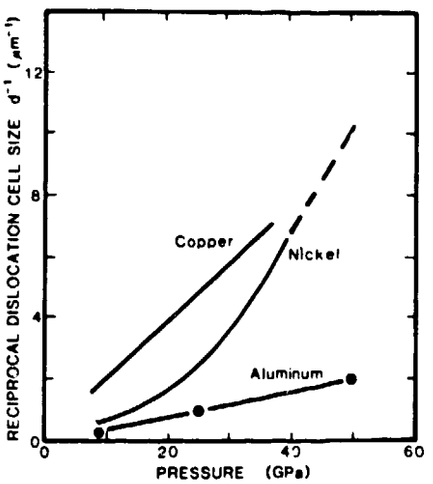

Fig. 6: Reciprocal dislocation cell size versus peak shock pressure for nickel, copper, and aluminum. Nickel and copper 2 μs pulse duration (11) and aluminum 1 μs pulse duration (32).

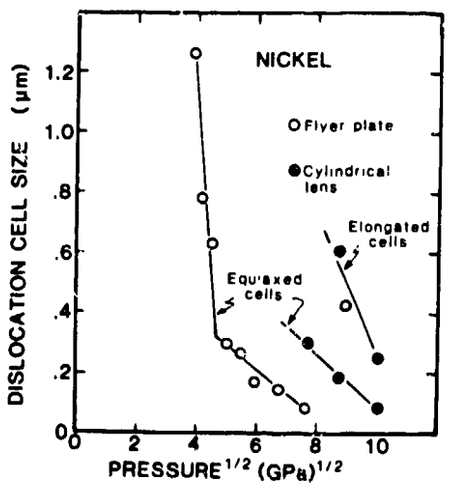

Fig. 7: Dislocation cell size versus square root of the peak pressure for nickel. Flyer plate data after Murr (11) and cylindrical lens explosion after Staudhammer (12).

D. Stacking fault energy and twinning: The stacking fault free energies of alloys depend upon the composition and temperature. For most low rate deformation processes the temperature component is of minor or negligible effect, while for shock rates, the temperature can have a major effect. The temperature effect becomes more dominant as the residual and strain heat increase, i.e., higher pressures. This effect is not uniform on all materials, as some materials have a negative dependence of stacking fault free energy and others a positive dependence with respect to temperature (24). Clearly, this aspect needs further research particularly in light of the higher pressures, strains and associated temperatures. Temperature affects aside, shock-loading of materials results in structure refinement. This

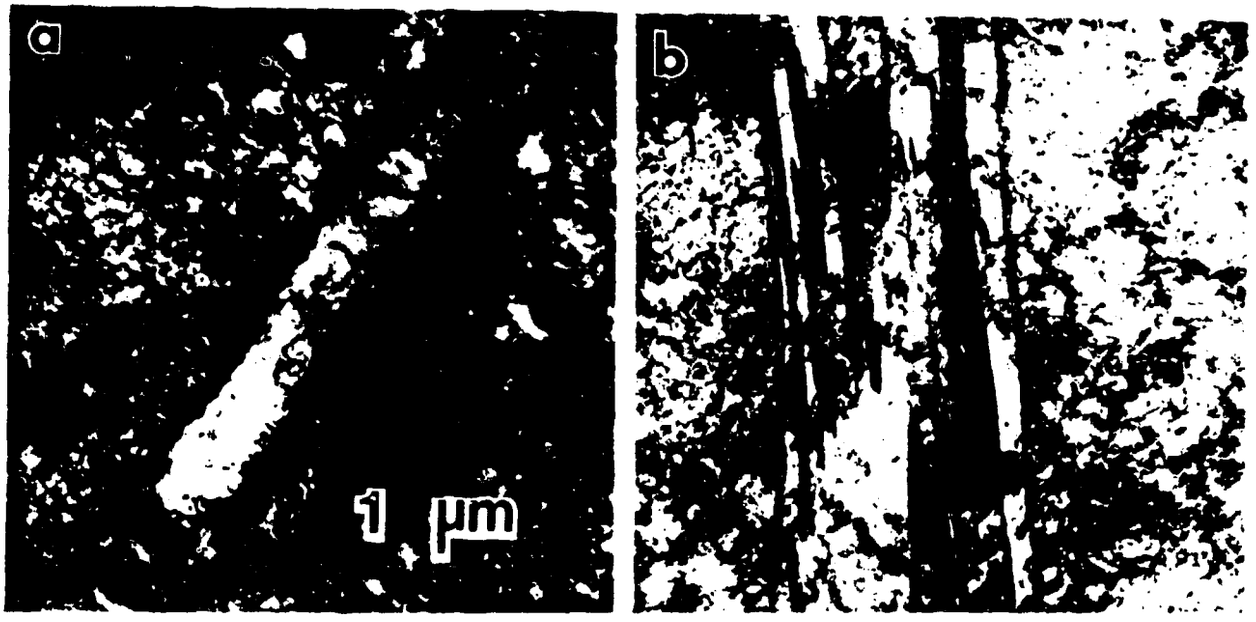

Fig. 8: Formation of a equiaxed and elongated cells and b) twins in 200 nickel shock loaded at 100 GPa.

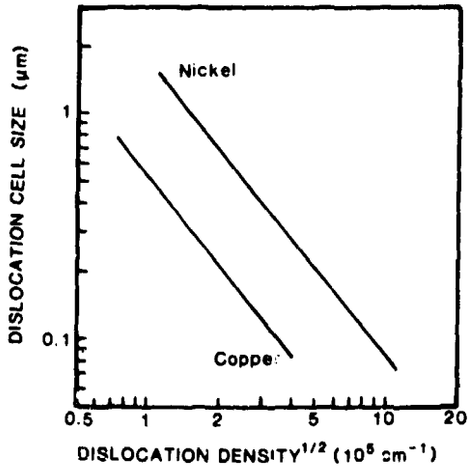

Fig. 9: Dislocation cell size versus square root of the dislocation density for shock loaded copper and nickel, after Murr (11).

effectively reduces the substructures size by planar intersecting arrays of dislocations, predominantly stacking faults or micro twins for low stacking fault free energy materials and by dislocation cells for high stacking fault free materials. All of the above, to varying degrees, can intermingle and produce twin-fault bundles for low stacking fault free energy materials as described by Staudhammer, et. al (37) and Johnson, et. al. (38). This has significant implications in martensitic transformations which will be discussed later.

Twinning in fcc materials is the result of overlapping intrinsic stacking faults or short segments of such faults due to the movement of groups of

dislocations on {111} planes. In bcc materials these {111} slip planes are not operative but move by somewhat different mechanisms involving groups of dislocation motion on other slip planes (33, 34). Consequently, one observes different twin morphologies in shock-loaded fcc materials as compared to bcc materials. On comparing twin structures obtained at lower pressures from data of Wongwiwat, et. al. (35) to somewhat higher pressures from data of Staudhammer, et. al. (36), the strain effect is very dominant and the sample fractures. A low twin volume of less than 10 percent was observed.

The relationship of twin fault volume to peak pressure was shown by Murr (11). In fcc materials, as the stacking fault energy decreases, the preponderence of twinning increases. This is shown in Figure 11. Concommitant with this decrease in stacking fault energy is a decrease in the onset of twinning; i.e., an increase in critical pressure for twinning is observed for higher stacking fault energy materials. Also effecting the data in Figure 11 is the preponderence for twinning as grain size increases.

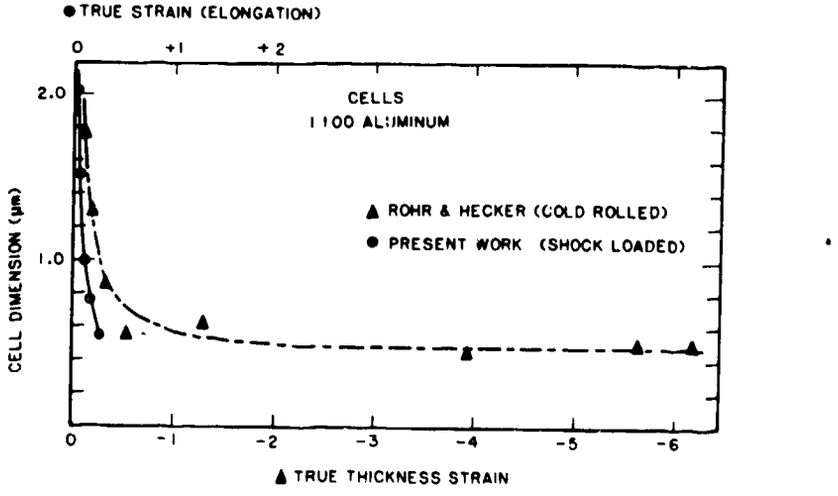

Fig. 10: Dislocation cell size versus true strain for shock loaded and cold rolled aluminum sheet. Cold rolled data after Rohr, et. al (13-15).

In some cases, systematically overlapping stacking faults can produce phase regions in addition to twin bundles. For example, ε (hcp) phase bundles (4) and with twin fault intersections, the formation of α'-martensite in 304 stainless steel (32).

Martensitic transformations can be induced by selective shear stesses or strains as more recently described by Staudhammer, et. al. (37) for 304 stainless steel. Numerous martensitic, as well as other transformations are reported in the literature. The topic of shock induced phase transformations warrants a chapter on its own and cannot adequately be discussed here.

E. Grain size: The effect of initial grain size on mechanical advantage (i.e., strengthening) follows a Hall-Petch relationship of the form:

$$\sigma = \sigma_o + KD^{-1/2}$$

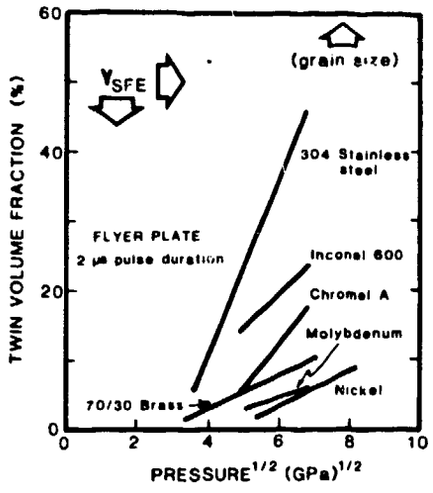

Fig. 11: Twin volume fraction versus square root of peak pressure for a number of metals and alloys, data after Murr (11).

where σ_o is the friction stress and in many instances the yield point of the material, K is a material constant and D is the average grain diameter. In shock loading similar effects are also observed in materials with cubic symmetry. In materials that do not exhibit cubic symmetry, individual grains have anisotropic compressibilities and hydrostatic stresses will establish compatibility stresses at their interfaces. It should be noted that the grain size is usually unchanged following shock loading. Consequently, grain size is not a direct contributor to strengthening. It does, however, contribute significantly to the residual substructure that develops which in turn affects the strengthening. For constant shock conditions, as grain size decreases, strengthening increases, and a constant grain size strengthening increases with increasing pressure (11) as shown in Figure 12. The residual substructures in molybdenum were shown (39) to be a function of grain size and that large grain sized specimens twinned more readily than small. Additional investigations have found similar results (40).

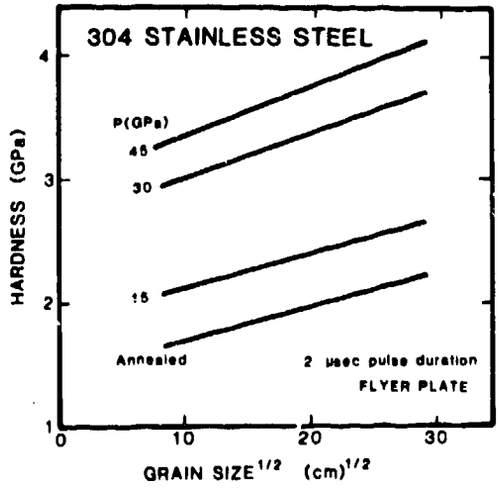

Fig. 12: Hardness versus square root of the dislocation density for 304 stainless steel shocked at various pressures. Correlation to the Hall-Petch relationship is evident. Data after Murr (11).

The Hall-Petch relationship can now be modified to include all the substructural features discussed here; which include twins, dislocations, dislocation cells, faults, twin-faults, etc. It should be pointed out that while all these substructural features contribute to a Hall-Petch effect, they are interactive and as such the magnitude of the contribution will be difficult to determine. For example, the change in slope noted in Figure 7 for nickel is due to a substructural change caused by the onset of twinning at pressures between 25 to 30 GPa. Consequently, dislocation cells are initially associated with shock strengthening while at higher pressures, twinning contributes. It should also be noted for the onset of twinning in nickel the associated strain is in excess of 15 percent, which can produce twinning by deformation and is not unique to shock loading.

Combined Effects

Material scientists know that the micro/macro-structure greatly influences the properties of a material. These properties are also a consequence of its thermo-mechanical history. Realizing this, one therefore carefully controls strains, temperatures of heat treatments, grain size and substructure, as well as strain rates and stress states. Ideally one tries to eliminate all but one variable. If this were possible, the field of shock response and material parameters would be better understood than it is today. Unfortunately, all of the material parameters discussed above are interdependent on one another to varying degrees, and with few exceptions difficult to isolate over the range of up to several megabars (100-200 GPa). Our tools for investigating residual shock effects on materials have become increasingly more sophisticated. However, in the realm of residual shock effects, these advanced techniques are often used to investigate the results of poorly designed experiments. Unfortunately, this produces results that are well quantified on uncertain conditions or histories. Conversely, the opposite is equally true. To cite an example of earlier work in the 50s which exemplifies this point, as stated by J. Taylor (41) "We're in the metallurgical mud".

Quite clearly, we need far more interdisciplinary crossover between physicists and material scientists. Still, if one looks back over the last 30 years or so, particularly in the last 10 years, one finds an enormous amount of metallurgical-material shock data.

A. Hardness: Hardness is one of the most widely used measurements that indicate microstructural modification by a shock event. Post hardness measurements reveal the total sum of all the shock-induced substructures discussed above, in addition to the pre-existing microstructure. In most instances hardness measurements can be considered an averaging process.

From a mechanical advantage point of view, hardness and subsequent increase in yield strength was first recognized as a major focal point in shock effects. This significant increase in hardness, by a factor of two in many cases concommitant with negligible dimensional changes make shock loading unique. Parameters which affect hardness, while contributive in nature, are also competitive as most mechanisms are dependent on dislocation generation, generation rate, movement and rearrangement.

Dislocations that split up into partials separated by a stacking fault interface are restricted to a single glide plane and can cross-slip only if

the partials recombine. For close packed crystals, cross-slip becomes increasingly difficult as the stacking fault free energy decreases. As a consequence of this, extended dislocations can harden intersecting slip systems by a grain refinement which occurs after strain has initiated dislocations and stacking faults, which have a tendency to form pileups extending across the grains, and in turn are intersected by other pile-ups and stacking faults. For high stacking-fault energy materials, the dislocations are mobile and are not measurably extended. Consequently, linear arrays are not favored and the formation of forest dislocation arrays results. These forest dislocations are transformed into sub-boundaries or dislocation cells. These dislocation cells constitute subgrain hardening similar to that of ordinary grain structures, except the effect is weaker and of shorter range.

In the case of overlapping stacking faults, particularly in fcc alloys, shock-loading can produce twinned or other phase transformed regions. The most prominent being the martensitic transformation in steel. In martensitic transformations, the resulting structure is strengthened by the interphase, as well as substructural refinement, which creates new interfaces to impede dislocation glide motion.

Typical hardness data for a low stacking fault material (i.e., 304 stainless steel) is shown in Figure 13. Many of the features referred to previously are encompassed in this material. The hardness initially increases at low pressures, peaks at close to 35 GPa and begins to decrease at approximately 80 GPa. This decrease at approximately 80 GPa has been attributed to shock heating effects. While shock heating effects are, in fact, more dominant at higher pressures one cannot exclude the strain heating effect which also dominates at higher pressures. This will be elaborated on in the next section using nickel as an example. The two curves shown in Figure 13 are examples from different experimental techniques. If one looks at the lower pressure regime (i.e., >40 GPa) and plots the hardness to the square root of the peak pressure, a straight line relationship is observed. This is shown in Figure 14 for a variety of materials. In this regime, the hardness is pressure-microstructure dominant. While heat effects occur,

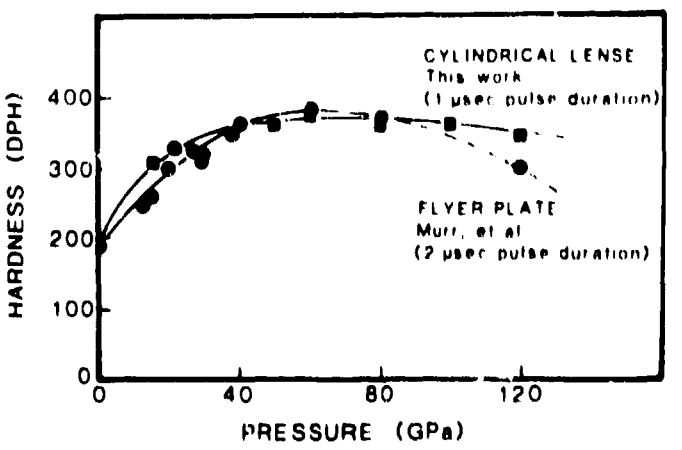

Fig. 13: Residual hardness versus pressure for 304 stainless steel. Comparison of flyer plate data after Murr (11) and cylindrical lense data.

relative to a homologous temperature, they are negligible. In this pressure range, hardness (H) can be described by the following equation:

$$H = H_o + n\sqrt{P} \qquad \text{Eq. (2)}$$

while H_o is the initial (annealed) hardness in GPa, P is the peak pressure and for fcc materials, and n is approximately 0.2. Attempts to rationalize the hardness data of Figure 14 to trends in stacking fault free energy, grain size, etc., proved inconclusive. Clearly more experimentation is needed. Figure 15 is an attempt to pull together the observed parameters that affect hardness for a number of materials.

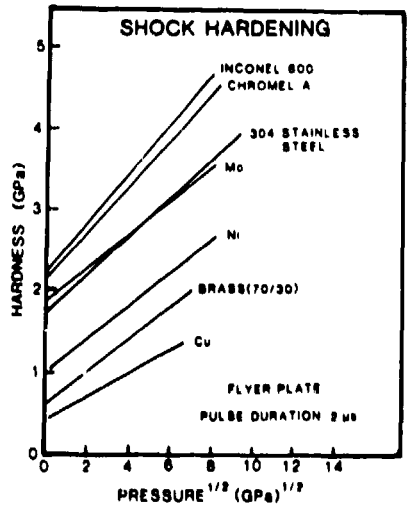

Fig. 14: Shock hardening in a variety of metals and alloys as a function of the square root of pressure. Data after Murr (11).

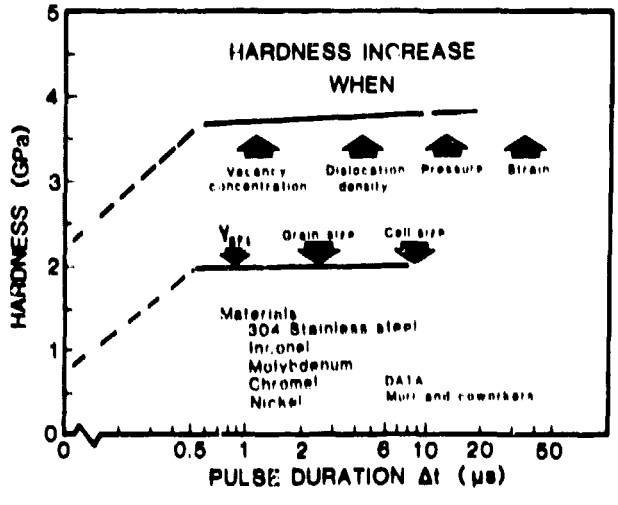

Fig. 15: Shock hardening in a variety of metals and alloys as a function of pulse duration. Arrows indicate hardness increase as a function of listed parameters. Data after Murr (19).

Hardness is essentially pulse-duration independent in the range of 0.5 to 14 us although some exceptions exist. For example, twinning and α'-martensite increase with pulse duration, however, no net gain in hardness is observed. The shock wave material parameters that increase hardness are shown in Figure 15. When stacking fault free energy, grain size and cell size decrease residual hardness is increased. Similarly, when vacancy concentration, dislocation density, pressure and strain increase, the residual hardness increases.

B. Strain and strain induced effects: With proper momentum trapping strain effects can essentially be eliminated in residual shock effects on materials. Unfortunately, inherent in most high pressure experiments (above 30 GPa) is the emergence of greater and greater strains as pressure increases. This increase in strain not only alters the microstructure by deformation, but concommitantly increases the temperature over and above the estimated residual temperature predicted by Rice et. al. (3). See Figure 2. The strain heat contribution is represented in Figure 16. Shown in this figure is the entropic heat at constant pressure obtained from Figure 2. This entropic heat is a calculated residual heat with no strain component. If the sample were allowed to strain at constant pressure, or strained as a result of exceeded design limitations, the sample would thus experience strain heating. Utilizing this concept, Staudhammer and Johnson (12, 30, 37, 42) were able to control strain and thus strain heating. For example, samples of 304 stainless steel shock loaded up to 170 GPa with an overall strain of 2 percent, were only warm to the touch within 1 minute after shock loading. On the other hand, similar samples shock loaded to 170 GPa with an overall strain of 26 percent, could not be touched even after 5 minutes. The technique for controlling strain, and thus minimizing the heating effects, is described in another paper in these proceedings by Staudhammer and Johnson.

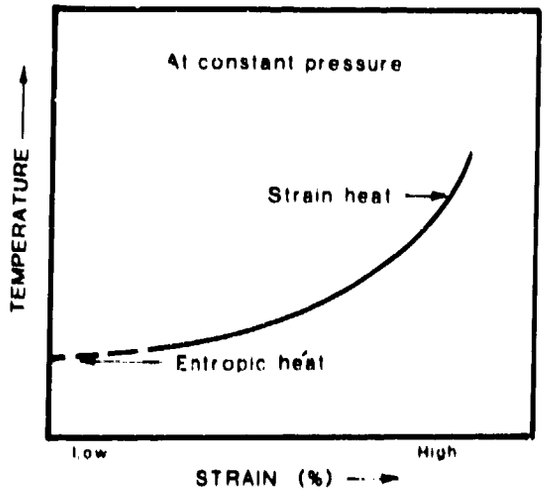

Fig. 16: Schematic representation of residual heat as a function of strain at a constant pressure. The entropic heat is equivalent to the ΔT_r in Fig. 2.

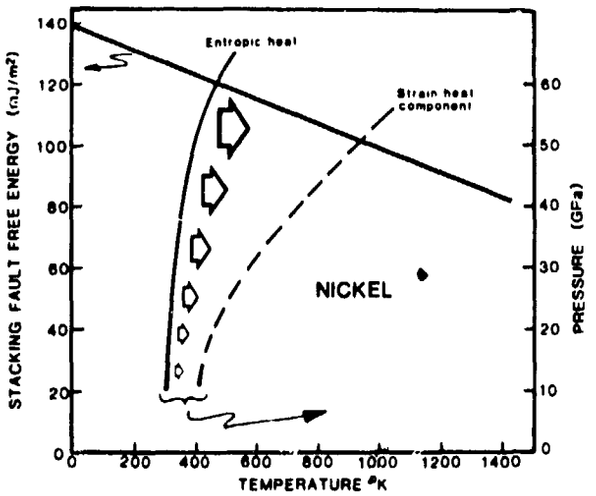

Fig. 19: Stacking fault energy decrease versus increase in temperature as a function of entropic and strain heat. Stacking fault free energy after (20) and entropic heat after (16).

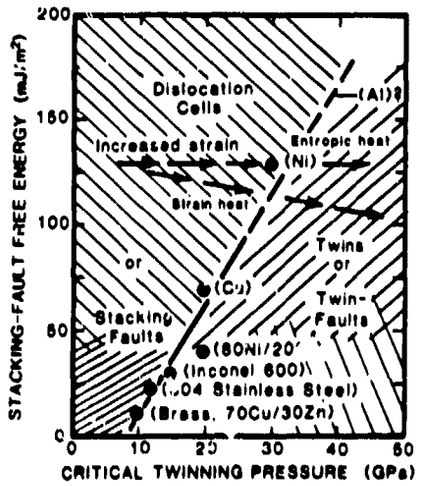

Fig. 20: Stacking fault free energy vs. critical twinning pressure for a number of materials. Illustration after Murr (37). Change in strain effect is superimposed on nickel relative to change in stacking fault free energy.

the same pressure with sufficient strain, which contributes an additional temperature increase of 400°K, would lower the stacking fault free energy by another 18 mJ/m^2. This drop in stacking fault free energy would decrease the propensity to form dislocation cells and promote twinning or twin faults. Indeed, similar anomolies were observed in nickel by Murr (23) at high pressures (approximately 10-14% strain), and Staudhammer and Johnson (36) at high pressures with 24 percent overall strain shown in Figure 8. This decrease in stacking fault free energy (strain induced) has an effect on the critical twinning pressure. This is shown in Figure 20. For a high stacking fault free energy material like nickel, the critical twinning pressure is more than twice that of 304 stainless steel. At this pressure, an increase in entropic heat, would only slightly shift the nickel data point down and to the right towards the twin or the twin-fault regime. However, with increased strain,

particularly with high pressures, the strain heat could drop the stacking fault free energy by as much as 20 percent and thus, easily shift the nickel data point from the cell dominated regime towards the twin or twin-faults regime. In spite of the limited data on nickel, clearly, the strain component does alter the residual microstructure. The question remains, though, whether or not twins in nickel, copper and even aluminum, would form at higher pressures if one were able to truly make a "strain free" test. Copper appears to be the best candidate for this as it has the lowest critical twinning pressure which in turn would have the lowest strain component to contend with. In addition, lowering the preshock temperature of the sample would help offset any small strain component of heat. To some extent this was done by Mogilevsky (17) on copper, though, primarily to retain residual microstructure, as well as to study low temperature effects.

Summary

In the present review, I have summarized results from some principal investigations of shock-strain effects in metals. The strain contribution indeed plays a role in residual microstructures, particularly, if the strain becomes dominant as in "under trapped" experiments of low or moderate pressure or for that matter, of "well trapped" high pressure experiments. Not only does this strain contribution affect the microstructure by increasing deformation, a concommitant strain heat is generated and absorbed by the shocked material. This strain heat, if large enough (relative to the homologous temperature of the material), can and does have an annealing effect on the residual microstructure. This strain heat is over and above the values typically calculated for materials implying little or no strain. Although the accumulative effects of associated strain are not completely definitive, the collective picture presented is one in which shock-induced strains, when large enough, have a significant effect on the residual microstructure.

Acknowledgements

The author wishes to acknowledge the support of ISRD and CMS funds from the Los Alamos National Laboratory over the years for research presented in this paper. In addition, I wish also to acknowledge the support and help of numerous colleagues in particular L. E. Murr and K. A. Johnson.

References

(1) J. S. Reinhart and J. Pearson: "Behavior of Metals Under Impulsive Loads", ASM, Cleveland, Ohio (1954).

(2) C. S. Smith: Trans. AIME 212 (1958) 574.

(3) M. H. Rice, R. G. McQueen and J. M. Walsh: "Compression of Solids by Strong Shock Waves, Solid State Physics", Academic Press, New York, Vol. 6, (1958).

(4) L. E. Murr and F. I. Grace: Exp. Mech., 5 (1969) 145.

(5) E. G. Zukas: Metals Engr. Quart. (ASM), 6 (1966) 16.

(6) W. C. Leslie: in "Metallurgical Effects at High Strain Rates", R. W. Rhode, et. al, eds., Plenum Press, New York (1973) 572.

(7) "Shock Waves and High-Strain-Rate Phenomena in Metals", M. A. Meyers and L. E. Murr, eds., Plenum Press, New York (1980).

(8) "Shock Waves in Condensed Matter - 1983", Proceedings of the American Physical Society Topical Conference, J. R. Asay, et. al., eds., North Holland, New York (1983).

(9) "Metallurgical Applications of Shock-Wave and High-Strain-Rate Phenomena", L. E. Murr, et. al., eds., Dekker, New York (1986).

(10) "Shock Waves in Condensed Matter", Y. M. Gupta, ed., Plenum Press, New York (1986).

(11) L. E. Murr in "Shock Waves and High-Strain-Rate Phenomena in Metals", M. A. Meyers and L. E. Murr, eds., Plenum Press, New York (1980) 607.

(12) K. P. Staudhammer, K. A. Johnson, and B. W. Olinger, "Proceed. of the 41st Annual Meeting of the Elect. Microscopy Soc. of America", San Francisco Press (1983) 272.

(13) D. L. Rohr and S. S. Hecker, Ninth International Congress on Electron Microscopy, Toronto, Vol. 1 (1978) 596.

(14) D. L. Rohr and S. S. Hecker, "39th Ann. Proc. Electron Microscopy Soc. Amer.", Claitors Pub. Co. (1981) 50.

(15) D. L. Rohr and S. S. Hecker, ibde (1981) 52.

(16) K. A. Johnson and K. P. Staudhammer: in "Metallurgical Applications of Shock-Wave and High-Strain-Rate Phenomena", L. E. Murr, et. al., eds., Dekker, New York (1986) 525.

(17) M. A. Mogilevsky and L. A. Teplyakova: in Metallurgical Applications of Shock-Wave and High-Strain-Rate Phenomena", L. E. Murr, et. al., eds., Dekker, New York (1986) 419.

(18) P. S. Follansbee, in "Metallurgical Applications of Shock-Wave and High-Strain-Rate Phenomena", L. E. Murr, et. al., eds., Dekker, New York (1986) 451.

(19) H. D. Kunze and L. W. Meyer, ibde, 481.

(20) Appendixes: in "Shock Waves and High-Strain-Rate Phenomena in Metals", M. A. Meyers and L. E. Murr, eds., Plenum Press, New York (1980) 1033.

(21) S. LaRouche and D. E. Mikkola, Scripta Met., 12 (1978) 543.

(22) R. N. Wright, et. al., in "Shock Waves and High-Strain-Rate Phenomena in Metals", M. A. Meyers and L. E. Murr, eds., Plenum Press, New York (1980) 703.

(23) L. E. Murr, in "Shock Waves and High-Strain-Rate Phenomena in Metals", M. A. Meyers and L. E. Murr, eds., Plenum Press, New York (1980) 753.

(24) L. E. Murr, "Interfacial Phenomena in Metals and Alloys", Addision-Wesly Pub.-Co., Inc. Reading, MA (1975).

(25) K. P. Staudhammer and L. E. Murr, Mat. Sci. and Engr. 44 (1980) 97.

(26) L. Davidson and R. A. Graham, Physics Reports 55 (1979) 256.

(27) J. J. Dick and D. L. Styris, J. Appl. Phys., 46 (1975) 1602.

(28) M. A. Mogilevsky "Combustion, Explosion, and Shock Waves", 6 (1970) 197.

(29) D. C. Brillhart, A. G. Preban, and P. Gordon, Met. Trans. 1 (1970) 969.

(30) K. P. Staudhammer and K. A. Johnson: "Proceedings of the International Symposium on Intense Dynamic Loading and Its Effects", C. M. Cheng and Ding Jing, eds., Science Press, Beijing, China (1986) 759.

(31) W. Zimmer, M. S. Thesis, New Mexico Inst. of Mining and Technology, Socorro, NM (1979).

(32) K. P. Staudhammer, S. S. Hecker, and L. E. Murr, Inter. Conf. on Solid-Solid Phase Transformations (1981) 1287.

(33) A. W. Sleeswyk, Mater. Sci. Engr. 30 (1977) 99.

(34) A. W. Sleeswyk, Phil. Mag. 3 (1963) 1469.

(35) K. Wongwiwat and L. E. Murr, Mater. Sci. Engr. 35 (1978) 273.

(36) K. P. Staudhammer and K. A. Johnson, unpublished data.

(37) K. P. Staudhammer, L. E. Murr, and K. A. Johnson, Acta Metall. 31, No. 2 (1983) 267.

(38) K. A. Johnson, L. E. Murr, and K. P. Staudhammer, Acta Metall. 33, No. 4 (1985) 677.

(39) L. E. Murr, O.T. Inal, and A. A. Morales, Appl. Phys. Letters, 28 (1976) 432.

(40) D. E. Duvall and R. A. Graham, Reviews of Modern Physics, 49 (1977) 523.

(41) J. W. Taylor, "Shock Waves in Condensed Matter - 1983", J. R. Asay, et. al., eds., North Holland (1983) 3.

(42) K. P. Staudhammer, K. A. Johnson, and B. Olinger, in "Shock Waves In Condensed Matter-1983", A. J. Asay, et. al., eds., Elsevier Sci. Pub. B. V. (1984) 419.

(43) L. E. Murr, "APS Topical Conference: Shock Waves in Condensed Matter", July 1987.